Modeling Sensorineural Hearing Loss, W. Jesteadt (Ed),
Lawrence Erlbaum Associates, February 1997

A Computational Model of Reorganization in Auditory Cortex in Response to Cochlear Lesions

Rick L. Jenison
University of Wisconsin, Department of Psychology
Madison, WI 53706

Running Head: **Model of Cortical Reorganization**

Address all correspondence to:

Rick L. Jenison, Ph.D.
Department of Psychology
University of Wisconsin
1202 West Johnson Street
Madison, WI 53706
Tel: (608) 262-9945
Fax: (608) 262-4029
E-mail: jenison@wavelet.psych.wisc.edu

ABSTRACT

Topographic representation or maps of sensory epithelia is a general feature throughout the brainstem and cortex. Recent evidence suggests that the maps may be labile and altered by use. Moreover, there is evidence that these topographic representations can be modified by lesioning regions of the peripheral receptor surface. Robertson and Irvine (1989) have examined the effects of partial unilateral cochlear lesions on the orderly topographic mapping of sound frequency in the auditory cortex of adult guinea pigs. They found that there is significant reorganization of the topographic representation following restricted damage to the cochlea. A self-organizing model of auditory cortex that incorporates biologically plausible neural mechanisms for reorganization will be presented. A computational model of the auditory periphery (Jenison, Greenberg, Kluender, & Rhode, 1991) drives the development of the self-organizing cortical model via exposure to a range of pure-tone frequencies. After the cortical model has "matured", the peripheral model is lesioned, and reorganization is allowed to proceed. Patterns of the reorganized frequency map are similar to those observed in the deafened adult guinea pigs. Possible mechanisms underlying the observed changes are discussed.

INTRODUCTION

Reorganization following partial peripheral dennervation and restricted natural stimulation has received considerable attention in the somatosensory system (Merzenich, Recanzone, Jenkins & Nudo, 1990). Less attention has been paid to reorganization in the auditory system in response to partial peripheral lesions, which could have significant implications for understanding the consequences of sensorineural hearing loss. Robertson and Irvine (1989) have demonstrated reorganization in primary auditory cortex in response to partial cochlear lesions that is similar in nature to that observed in somatosensory cortex.

In this chapter, the behavior of a computational model of cortical reorganization to patterns generated by a computational model of a notch-lesioned cochlea is examined. The pattern of reorganization may provide insights into possible frequency representations for specific forms of sensorineural hearing impairment. The ability to computationally explore these patterns may have implica-

tions for the design of signal processing strategies for hearing aids and cochlear implants.

ORGANIZATION OF AUDITORY CORTEX

The auditory system exhibits widespread convergence and divergence of information that is accomplished primarily within the confines of the tonotopic map which runs approximately rostrocaudally across the surface of AI in cat (Merzenich, Jenkins & Middlebrooks, 1984). In register with the cochleotopic map may be other functional organizations representative of computations carried out along the auditory pathway. Neurons with similar preferred or characteristic frequencies are organized into narrow, parallel "isofrequency" bands that run dorsoventrally across the surface of AI. Hence, isofrequency bands are composed of neurons that respond best to input from a restricted region of cochlear place. Organization within isofrequency bands may include gradients of frequency tuning in cat (Schreiner & Sutter, 1992), intensity sensitivity (Heil, Rajan, & Irvine, 1994), and receptive field shape (Shamma, Fleshman, Wiser, & Versnel, 1993).

PLASTICITY IN SENSORY MAPS

Structural and functional changes of the sensory cortices appear to occur throughout the lifetime of many animals (Merzenich et al., 1990), including changes observed in primary auditory cortex of adult owl monkeys (Recanzone, Schreiner, & Merzenich, 1993), macaque monkeys (Schwaber, Garraghty, & Kaas, 1993), and cat (Rajan, Irvine, Wise, & Heil, 1993). The relative roles of afferent input and the cortical targets in forming sensory maps has been investigated by Sur and colleagues (Roe, Pallas, Hahm & Sur, 1990) by surgically redirecting retinal inputs into the auditory pathway of ferrets. Remarkably, primary auditory cortex contained a systematic representation of visual space rather than a tonotopic frequency representation, suggesting that the same cortical area can support different types of organization. There are two possible mechanisms that have been proposed to account for plasticity in the central nervous system - growth of connections and change in the effectiveness of existing connections (Kaas, 1991). The rapidity with which these changes occur implicates the latter as the dominant mechanism. However, early in development, significant axonal remodeling of the thalamocortical patches within AI appears to take place, suggesting the possibility of activity-dependent refinement of structural arborization to target neuron dendrites (de Venecia &

McMullen, 1994).

SELF-ORGANIZING NEURAL NETWORKS

There have been several models for activity-dependent development of cortical maps, using so-called unsupervised learning strategies based on Hebbian learning. Hebbian learning refers to synaptic modification where a synapse (or connection) is strengthened when there is correlation between presynaptic and postsynaptic activation or depolarization, and weakened when there is uncorrelated activity. One proposed physiological correlate of Hebbian learning is that of long-term potentiation of synaptic effectiveness mediated by NMDA receptors. Mediation by NMDA receptors has been implicated in ocular dominance plasticity in the visual cortex (Kleinschmidt, Bear, & Singer, 1987). Computational neural network models that abstractly express these mechanisms have demonstrated how global topographic order can emerge, in principle, from local cooperative and competitive interactions within a cortical structure. Many of these models have focused on problems of vision, beginning with the work of von der Malsburg (1973) on the development of orientation selectivity in visual cortex. More recently, Miller (1994) has studied correlation-based mechanisms in the visual system with unsupervised models, which are consistent with the modeling effort described in this chapter.

Local enhancement of cell activity is thought to be mediated by lateral cortical connections. Lateral feedbacks in the aforementioned models are assumed to be excitatory at short lateral distances and inhibitory at longer lateral distances. Although long-range intracortical projections have been observed anatomically, evidence that more distant connections are inhibitory is inconclusive (Gilbert, Hirsch, & Wiesel, 1990). A simplified neuron in such a network model can be mathematically characterized as a nonlinear differential equation where the magnitude of the mathematical function output can be thought of as the strength of response of the cell.

SELF-ORGANIZING MODEL OF AUDITORY CORTEX

The cortical model, used in the simulations presented here, is an abstract representation of activity on a 2-dimensional surface dependent on ascending afferent input (see Figure 1). This highly simplified representation ignores, for the time being, the third dimension of cortical layers and biophysical detail. Neighboring regions on this dynamic, plastic surface have the capacity to develop

similar features, including emergent properties such as systematic organization of intensity sensitivity, bandwidth, spectral shape, and binaural properties (when receiving input from both ears).

INSERT FIGURE 1

Lateral connections in the two-dimensional sheet are defined by two Gaussian functions that depend on the anatomical cortical distance ($\|r - r'\|$) between any two "cells", r and r', on the cortical sheet. The combined excitation E (solid lines) and inhibition I (dashed lines) result in the following Difference of Gaussians (DOG), or Mexican-Hat function describing the intracortical interaction between anatomically neighboring cells:

$$E(r,r') = \frac{1}{\sqrt{2\pi s_E^2}} e^{\left[-\frac{(r - r')^2}{2s_E^2}\right]} \text{ and } I(r,r') = \frac{1}{\sqrt{2\pi s_I^2}} e^{\left[-\frac{(r - r')^2}{2s_I^2}\right]} \quad (1)$$

where $G(r,r') = \alpha E(r,r') - \beta I(r,r')$. s_I and s_E determine the intracortical range of excitation and inhibition, and α and β are relative gain terms. The response η_{ij} for any cortical neuron r_{ij} in the sheet can then be described by the following nonlinear difference equation

$$\eta_{ij} = f\left(\sum_k c_{ijk} w_{ijk} v_k + \sum_{mn} G(r_{ij}, r_{mn})\, \eta_{mn}\right) \quad (2)$$

where f is a compressive nonlinear transform. The input vector $\cdot$ corresponds to an array of responses from ascending afferents indexed by k. In this model, ascending axons project to selective cortical neurons determined by a connection or arborization matrix c_{ijk}. Changes in the afferent weights (synapses) w_{ijk} take place via local Hebbian (correlative) learning, starting with random assignments. Equation 2 is numerically integrated (iterated) following each stimulus presentation until it reaches a state of equilibrium, that is, a state where the system is no longer changing. From this complex interaction emerges a region of common cortical activity dependent on the ascending pattern of activity. After Equation 2 reaches equilibrium, each w_{ijk} is updated with the following Hebbian rule:

$$w_{ijk}(t+1) = \frac{c_{ijk} w_{ijk}(t) + \varepsilon(t)\, \eta_{ij} \nu_k}{\sum_k \left[c_{ijk} w_{ijk}(t) + \varepsilon(t)\, \eta_{ij} \nu_k \right]} \quad (3)$$

Afferent weights are strengthened when the afferent pattern of activity is correlated with cortical activity η_{ij} and weakened when uncorrelated. As the afferent weights change over time *t* through repeated exposure to afferent pattern ˙, the learning rate ε decreases, and the neighborhood defined by s_E in the Mexican-Hat function is systematically reduced in size over time. The narrowing of lateral effectiveness of cortical neurons appears to be a necessary modeling constraint for the refinement of afferent weights, and is intended to reflect developmental processes. Although yet to be shown in auditory cortex, refinement of intracortical clusters has been demonstrated in visual cortex (Callaway & Katz, 1990).

APPROXIMATING AUDITORY NERVE RESPONSES

For this computational study, ascending afferent input was generated by a computational model of the auditory nerve (AN) that we developed several years ago (Jenison, Greenberg, Kluender & Rhode, 1991). Pure-tone stimuli are transformed into spectral-place patterns of AN activity, commonly referred to as the peripheral excitation pattern. This particular model is a member of a class of auditory periphery models that are considered to be functional in nature (e.g., Patterson & Holdsworth, 1991; Lyon, 1991; Seneff, 1988). In this case, the goal of the modeling effort is to functionally approximate the input-output behavior of the cochlea, without advancing a parametric biomechanical model of the basilar membrane. The goal of the Jenison et al. model was to faithfully approximate the change in frequency selectivity of single auditory nerve fibers over a range of intensities. Filter functions were derived from average-rate iso-intensity functions of 97 cat high spontaneous-rate auditory-nerve fibers (see example in Figure 2), and were thus based directly on physiological filter properties, in so far as they are reflected in the rate response of single fibers. The average-rate isointensity function of single fibers is assumed to reflect the summed filtering effects of mechanical basilar membrane (BM) tuning, inner hair cell (IHC) transduction, IHC neurotransmitter release, and auditory nerve spike generation. Thus, all varieties of nonlinearities such as BM

compression, IHC receptor potential saturation, spike rate saturation of the AN, thresholding, etc. are reflected in the output response of auditory-nerve fibers. The pattern of excitation of 128 modeled AN fibers in response to pure-tones at two intensity levels are shown in Figure 3. Each curve represents the cochleotopic array of AN responses to a single tone.

INSERT FIGURES 2 & 3

LESIONING THE AUDITORY NERVE MODEL

The functional auditory-nerve model can be "damaged" by modifying the nonlinear filtering characteristics of the model, an approach inspired by Allen (1991) in modeling noise damaged stereocilia of the cochlea. The approach involves inducing elevated auditory-nerve threshold tuning curve tips and downward-shifts in characteristic-frequency based on observations of auditory nerves from damaged cochleas (Liberman, 1984; Liberman & Dodds, 1984). While it is straightforward to make the necessary modifications to the normal auditory periphery model, an alternative approach would be to approximate isointensity functions directly from auditory nerve recordings from a damaged cochlea.

A simulated compound action potential (CAP) audiometric function (see Johnstone, Alder, Johnstone & Yates, 1979) is shown in Figure 4 before and after lesioning of the auditory-nerve model. The CAP function reflects the sum status of the receptors and auditory nerve fibers at each of the test frequencies presented, and is used to match the modeled lesion to that induced in the guinea pig by Robertson and Irvine.

INSERT FIGURE 4

SIMULATION OF FREQUENCY REORGANIZATION

In the Robertson and Irvine study, restricted lesions in adult guinea pigs immediately resulted in highly elevated thresholds for cortical neurons along the tonotopic axis that normally represented the damaged region of the cochlea. One to three months following the lesion, the region of cortex that previously possessed high-thresholds corresponding to the lesioned cochlear regions, now had

normal thresholds, but at those frequencies adjacent to the frequency range damaged by the lesion.

In the computational modeling study, the ascending cochleotopic excitation pattern, ostensibly expressed at the level of the thalamus (ventral medial geniculate nucleus, vMGB), served as the input to the self-organizing model. The excitation pattern was derived from the auditory-nerve model transformed for an average-sized guinea pig cochlea using the frequency-position formula and parameters described by Greenwood (1990). This transformation was made to reflect the relative warping and range of frequencies encoded by the guinea pig cochlea.

The architecture was constructed as shown in Figure 1, with 32 cells along the rostrocaudal (tonotopic) axis and 30 cells along the dorsoventral (isofrequency) axis. The restricted afferent terminal arborization of approximately 500 μm is based on observed thalamocortical terminal patches in layer III and IV of the rabbit (de Venecia & McMullen, 1994). Development of the network then proceeded whereby the afferent connection weights w_{ijk} were modified based upon experience. The network was exposed to many presentations of differing frequencies (ranging from 100 Hz - 35 kHz) and intensities (ranging from 10 - 80 dB SPL) represented by the excitation pattern of the peripheral model. In order to simulate the incremental development of the basilar membrane from base to apex (Rubel, 1984), modeled excitation patterns are progressively shifted from base to apex during the development of the modeled cortex. In these simulations, only the strength of ascending afferent connections are modified based on Hebbian learning. The intracortical connections were systematically modified over time, but always constrained to the DOG pattern of excitation and inhibition, as described earlier. Figure 5 shows the initial condition of the connection weights mapped from distance along the BM frequency-position axis to location along the rostrocaudal axis in primary auditory cortex. The fixed terminal arborization (connectivity pattern) reflecting the afferent range of projection schematized in Figure 1 is expressed as the diagonal band, and the initial random strengths of connection weights are denoted by the gray scale within the band. Development then proceeds with several thousand presentations of random frequencies and intensities using an intact auditory nerve model (normal CAP audiometric function). The resulting “mature” connection strengths are shown in Figure 6. Note that the connection weights are no longer random, but show smooth refinement within the arborization. The resultant response areas of cortical cells along the

rostrocaudal axis of the simulated mature cortex in response to systematic steps in pure-tone frequencies are shown in Figure 7. Superimposed on the gray-scaled response areas of the simulated cortex (darker represents higher discharge rates) are the characteristic-frequencies of cortical cells from animal 86-56 from the Robertson and Irvine study, showing a relatively close correspondence to the peaks of the modeled responses.

INSERT FIGURES 5,6, &7

The next step was to lesion the modeled cochlea by decreasing the sensitivity and downward shifting the characteristic-frequency of auditory-nerve fibers in the restricted range of 10 - 20 kHz. The simulated postlesion CAP audiometric function is shown as the dotted line in Figure 4. This CAP function approximates that of animal 86-57 in the Robertson and Irvine study. The resulting cortical isointensity response areas, immediately postlesion, are shown in Figure 8. Reduced activity is observed in the region of the cortex corresponding to the lesioned ascending afferents, approximately 1.4 - 2.2 mm from the rostral edge, which corresponds to the gap predicted from the lesioned excitation pattern.

The cortical network was then allowed to reorganize to the lesioned cochlea, as a consequence of further random presentations of acoustic stimuli. During the recovery phase, the range of lateral intracortical connections are preserved in the “mature” state, maintaining relatively short-range intracortical interactions. However, afferent connection weights are allowed to update using previously described Hebbian learning. The resulting cortical activity is shown in Figure 9. Superimposed on the gray-scale map are the characteristic-frequencies of animal 86-57 following 35 days of recovery. It is apparent in both the modeled cortex, as well as the with the physiological data, that the low characteristic-frequencies are consistent with the pre-lesion condition. However, there is now a large region of cortex (600-700 μm) preferentially responding to frequencies around 10 kHz (i.e. the lower edge of the cochlear lesion). A similar effect can be observed for the upper edge of the cochlear lesion near 20 kHz. The model demonstrates a slightly more complete expanded representation into the region deprived of its normal input than that observed in the physiology. The ascending afferent

weights of the model following the recovery period are shown in Figure 10. While connection strength remains comparable to that of the intact cochlea for low characteristic-frequencies, the connection weights in the region of the lesion have markedly changed. Specifically, the connection weights projecting from those frequencies near the edge of the lesion have strengthened, and those in the region of the lesion have weakened.

INSERT FIGURES 8, 9, & 10

DISCUSSION

The results of both the physiological and modeling studies suggest that following restricted damage to the cochlea there is a functional reorganization of the representation of characteristic-frequency along the rostrocaudal (tonotopic) axis of auditory cortex. The model offers a possible explanation as to how long-term cortical expansion might occur, based on simple local Hebbian modification of connection weights. Immediately after the cochlear lesion, the afferent connection weights have not had time to change, hence those connections reflecting the lesioned regions of the periphery are “quiet” and a gap in the cortical tonotopic map is observed. The region of cortex deprived of ascending afferent input will now have less inhibitory effect on neighboring regions, allowing those regions to increase their strength of response. This heightened activity near the deprived edge will be correlated with those connections from active regions of the basilar membrane, hence strengthening the driving afferents and weakening those originating from the lesioned region. As a consquence of the dynamic lateral interactions, a common frequency representation progressively expands from the edge frequencies into the region that previously represented the now lesioned frequencies. Figure 10 illustrates the outcome of this self-organizing process, where the connection weights have weakened in the cochleotopic region of lesioned frequencies (on the ordinate), but strengthened at the edge frequencies which project to the region of cortex previously responding to the lesioned frequencies (on the abscissa). The range of possible reorganization appears to be determined in the modeling study by the range of terminal arborization, about 600-700 μm. A similar range is also observed in the physiological study. An important finding of the compu-

tational study is the observation of functional reorganization without physical rewiring (sprouting/pruning) of the afferent projections, instead reorganization occurs through local interactions inducing synaptic change.

The ability of this dynamical model to accurately simulate patterns of reorganization to peripheral sensorineural lesions in animal models may hold some promise for a better understanding of possible functional reorganization of central representations in human sensorineural impaired populations. Future directions include exploring reorganized cortical topographies induced by specific models of auditory-nerve responses to electrical stimulation (see for example Finley, Wilson, & White, 1990).

FIGURE CAPTIONS

Figure 1. Architecture for self-organizing model of auditory cortex. The rostrocaudal axis is constrained to be coarsely tonotopic by restricted connectivity to the cochleotopic ascending afferents. Lateral connections between cortical cells can be excitatory (solid lines) or inhibitory (dashed lines).

Figure 2. Isointensity functions for a single auditory-nerve fiber from the cat.

Figure 3. Excitation pattern generated by the auditory-nerve model as a function of position. Bold lines represent pure-tone responses at 80 dB SPL. Narrow lines represent 35 dB SPL.

Figure 4. Simulated CAP audiometric function. Solid line represents intact auditory-nerve model. Dotted line represents the lesioned auditory-nerve model.

Figure 5. Connection pattern (terminal arborization) and relative connection strengths from cochleotopic excitation pattern generated by the auditory-nerve model to a single row of cortical cells along the rostrocaudal axis. Connection weights are initially random. Darker squares represent stronger connections.

Figure 6. Connection pattern (terminal arborization) and relative connection strengths from cochleotopic excitation pattern generated by the auditory-nerve model to a single row of cortical cells along the rostrocaudal axis following development to maturity. Darker squares represent stronger connections.

Figure 7. Isointensity (50 dB SPL) response areas for a single row of cortical cells along the rostrocaudal axis following development to maturity with an intact cochlea. The darker areas represent stronger responses. The circles denote the CFs of animal 86-56 from Robertson and Irvine (1989).

Figure 8. Isointensity (50 dB SPL) response areas for a single row of cortical cells along the rostrocaudal axis immediately following the notch lesion shown in Figure 4. The darker areas represent stronger responses.

Figure 9. Isointensity (50 dB SPL) response areas for a single row of cortical cells along the rostrocaudal axis following recovery to the notch lesion shown in Figure 4. The darker areas represent stronger responses. The circles denote the CFs of animal 86-57 from Robertson and Irvine (1989).

Figure 10. Connection pattern (terminal arborization) and relative connection strengths from cochleotopic excitation pattern generated by the auditory-nerve model to a single row of cortical cells along the rostrocaudal axis following recovery to the notch lesion shown in Figure 4. Darker squares represent stronger connections.

REFERENCES

Allen, J. B. (1990). Modeling the noise damaged cochlea. In P. Dallos, C. D. Geisler, J. W. Mathews, M. A. Rugerro & C. R. Steele (Eds.), Mechanics and Biophysics of Hearing (pp. 324-331). New York: Springer-Verlag.

Callaway, E. M. & Katz, L. C. (1990). Emergence and refinement of clustered horizontal connections in cat striate cortex. Journal of Neuroscience, 10, 1134-1153.

de Venecia, R. K. & McMullen, N. T. (1994). Single thalamocortical axons diverge to multiple patches in neonatal auditory cortex, Developmental Brain Research, 81, 135-142.

Finley, C. C., Wilson, B. S. & White, M. W. (1990). Models of neural responsiveness to electrical stimulation. In J. M. Miller & F. A. Spelman (Eds.) Cochlear implants: models of the electrically stimulated ear. (pp. 55-92). New York:Springer-Verlag.

Gilbert, C. D., Hirsch, J. A., & Wiesel, T. N. (1990). Lateral interactions in visual cortex. Cold

Spring Harbor Symposia on Quantitative Biology, 60, 663-677.

Greenwood, D. D. (1990). A cochlear frequency-position function for several species - 28 years later. Journal of the Acoustical Society of America, 87, 2592-2605.

Heil, P., Rajan, R. & Irvine, D. R. F. (1994). Topographic representation of tone intensity along the isofrequency axis of cat primary auditory cortex. Hearing Research, 76, 188-202.

Jenison, R. L., Greenberg, S., Kluender, K. R. & Rhode, W. S. (1991). A composite model of the auditory periphery for the processing of speech based on the filter response functions of single auditory-nerve fibers. Journal of the Acoustical Society of America, 90, 773-786.

Johnstone, J. R., Alder, V. A., Johnstone, B. M., Robertson, D. & Yates, G. K. (1979). Cochlear action potential threshold and single unit thresholds. Journal of the Acoustical Society of America, 65, 254-257.

Kaas, J. H. (1991). Plasticity of sensory and motor maps in adult animals. Annual Review of Neuroscience, 14, 137-167.

Kleinschmidt, A., Bear, M. F. & Singer, W. (1987). Blockade of 'NMDA' receptors disrupts experience-dependent plasticity of kitten striate cortex. Science, 238, 355-358.

Liberman, M. C. (1984). Single-neuron labeling and chronic cochlear pathology. I. Threshold shift and characteristic-frequency shift. Hearing Research, 16, 33-41.

Liberman, M. C. & Dodds, L. W. (1984). Single-neuron labeling and chronic cochlear pathology. III. Stereocilia damage and alterations of threshold tuning curves. Hearing Research, 16, 55-74.

Lyon, R. F. (1991). Automatic gain control in cochlear mechanics. In P. Dallos, C. D. Geisler, J. W. Mathews, M. A. Rugerro & C. R. Steele (Eds.), Mechanics and Biophysics of Hearing (pp. 395-402). New York: Springer-Verlag.

Merzenich, M. M., Jenkins, W. M. & Middlebrooks, J. C. (1984). Observations and hypotheses on special organizational features of the central auditory nervous system. In G. M. Edelman, W. E. Gall and W. M. Cowan (eds.) Dynamic aspects of neocortical function (pp. 397-424). New York: Wiley.

Merzenich, M. M., Recanzone, G. H., Jenkins, W. M.& Nudo, R. J. (1990). How the brain functionally rewires itself. In M. Arbib and J. A. Robinson (Eds.), Natural and Artificial Parallel Com-

putations (pp. 177-210). Cambridge, MA: MIT Press.

Miller, K. D. (1994). A model of the development of simple cell receptive fields and the ordered arrangement of orientation columns through activity-dependent competition between ON- and OFF-center inputs. Journal of Neuroscience, 14, 409-441.

Patterson, R. D. & Holdsworth, J. (1991). A functional model of neural activity patterns and auditory images. In W. A. Ainsworth (Ed.), Advances in Speech, Hearing and Language Processing (in press) London: JAI.

Rajan, R., Irvine, D.R.F., Wise, L.Z., & Heil, P. (1993). Effect of unilateral partial cochlear lesions in adult cats on the representation of lesioned and unlesioned cochleas in primary auditory cortex. Journal of Comparative Neurology, 338, 17-49.

Recanzone, G. H., Schreiner, C. E. & Merzenich, M. M. (1993). Plasticity in the frequency representation of primary auditory cortex following discrimination training in adult owl monkeys. Journal of Neuroscience, 13, 87-103.

Robertson, D. & Irvine, D. R. F. (1989). Plasticity of frequency organization in auditory cortex of guinea pigs. Journal of Comparative Neurology, 282, 456-471.

Roe, A. W., Pallas, S. L., Kwon, Y. H. & Sur, M. (1992). Visual projections routed to the auditory pathway in ferrets: receptive fields of visual neurons in primary auditory cortex. Journal of Neuroscience, 12, 3651-3664.

Rubel, E. W. (1984). Ontogeny of auditory system function. Annual Review of Physiology, 46, 213-229.

Schreiner, C. E. & Sutter, M. L. (1992). Topography of excitatory bandwidth in cat primary auditory cortex: single-neuron versus multiple-neuron recordings. Journal of Neurophysiology, 68, 1487-1502.

Schwaber, M. K., Garraghty, P.E., and Kaas, J.H. (1993). Neuroplasticity of the adult primate auditory cortex following cochlear hearing loss. American Journal of Otology, 14, 252-258.

Seneff, S. (1988). A joint synchrony/mean-rate model of auditory speech processing. Journal of Phonetics, 16, 55-76.

Shamma, S. A., Fleshman, J. W., Wiser, P. R. & Versnel, H. (1993). Organization of response areas in

ferret primary auditory cortex. Journal of Neurophysiology, 69, 367-383.

von der Malsburg, C. (1973). Self-organization of orientation selective cells in the striate cortex. Kybernetik, 14, 85-100.

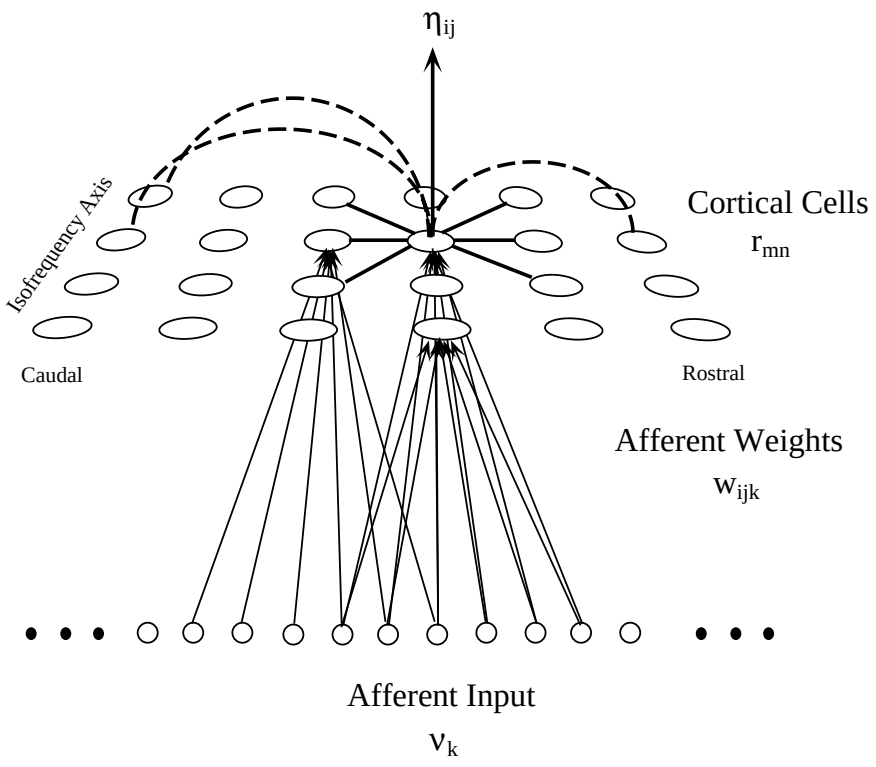
η_{ij}
Isofrequency Axis
Cortical Cells
r_{mn}
Caudal
Rostral
Afferent Weights
w_{ijk}
Afferent Input
ν_k

FIG. 1

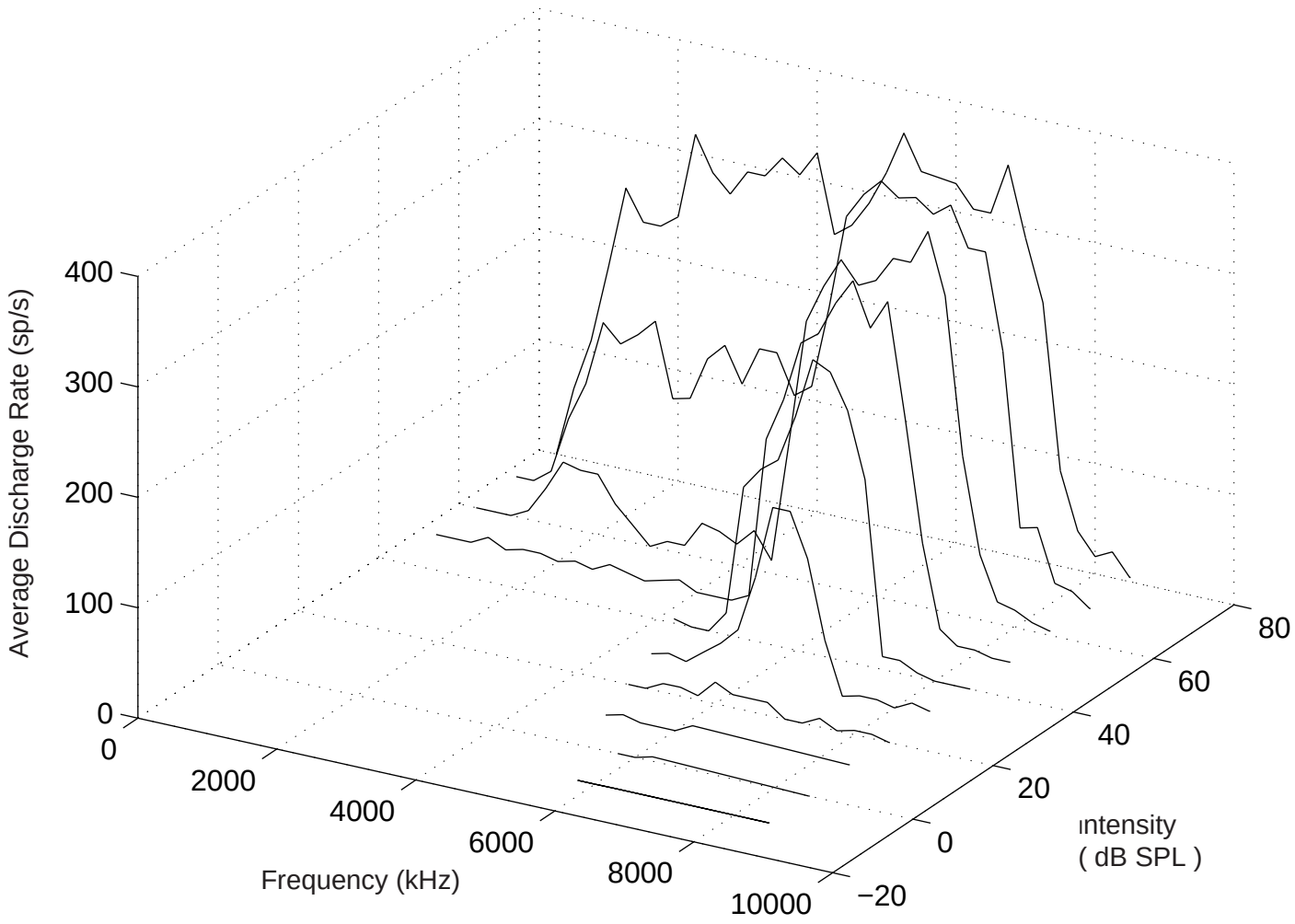
Average Discharge Rate (sp/s)
400
300
200
100
0
0
2000
4000
6000
8000
10000
Frequency (kHz)
80
60
40
20
0
−20
ıntensity
(dB SPL)

FIG. 2

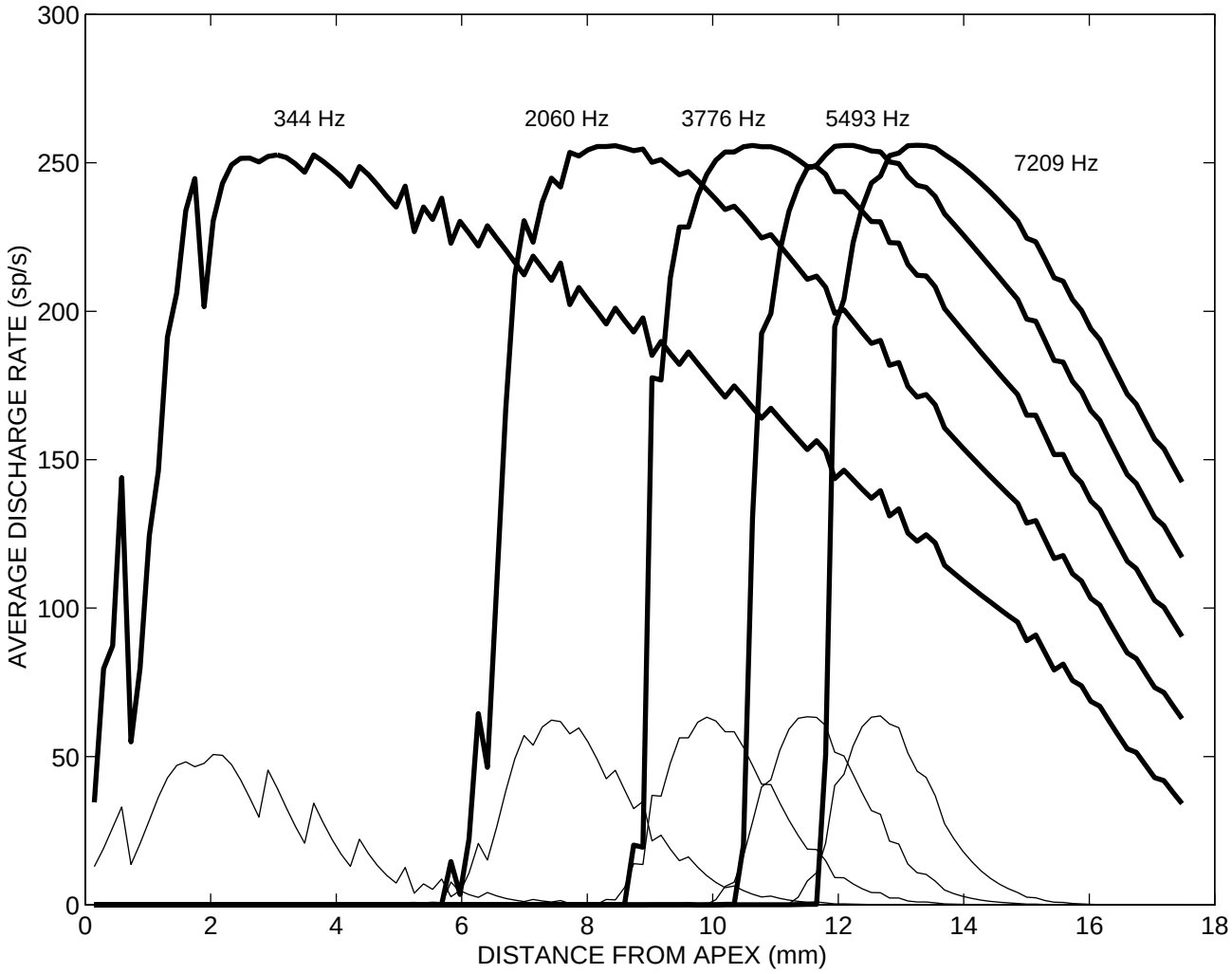
300
250
200
150
100
50
0
0
2
4
6
8
10
12
14
16
18
AVERAGE DISCHARGE RATE (sp/s)
DISTANCE FROM APEX (mm)
344 Hz
2060 Hz
3776 Hz
5493 Hz
7209 Hz

FIG.3

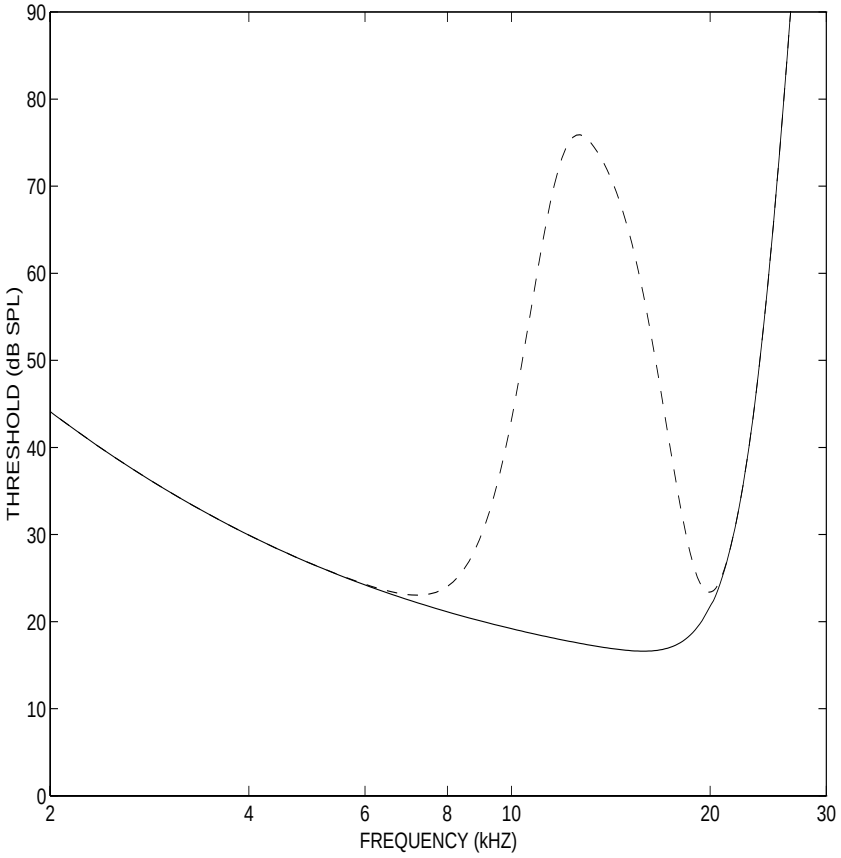
90
80
70
60
50
40
30
20
10
0
THRESHOLD (dB SPL)
2
4
6
8
10
20
30
FREQUENCY (kHZ)

FIG.4

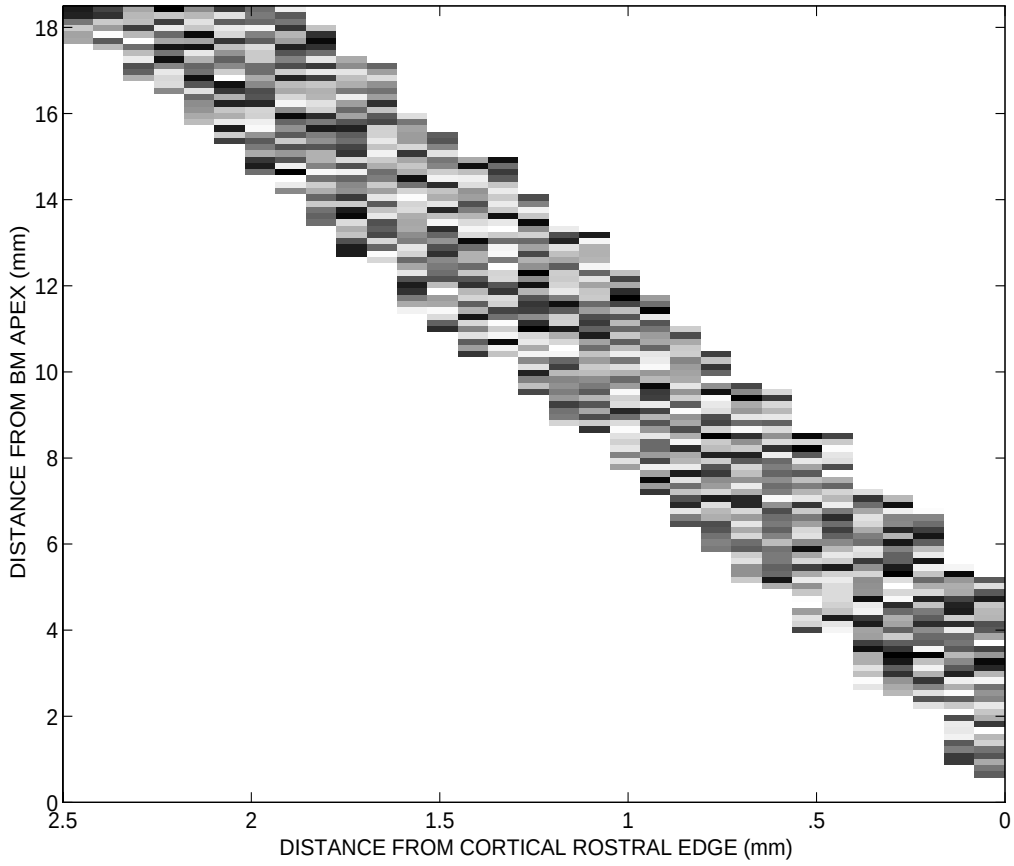
DISTANCE FROM BM APEX (mm)
0
2
4
6
8
10
12
14
16
18
2.5
2
1.5
1
.5
0
DISTANCE FROM CORTICAL ROSTRAL EDGE (mm)

FIG.5

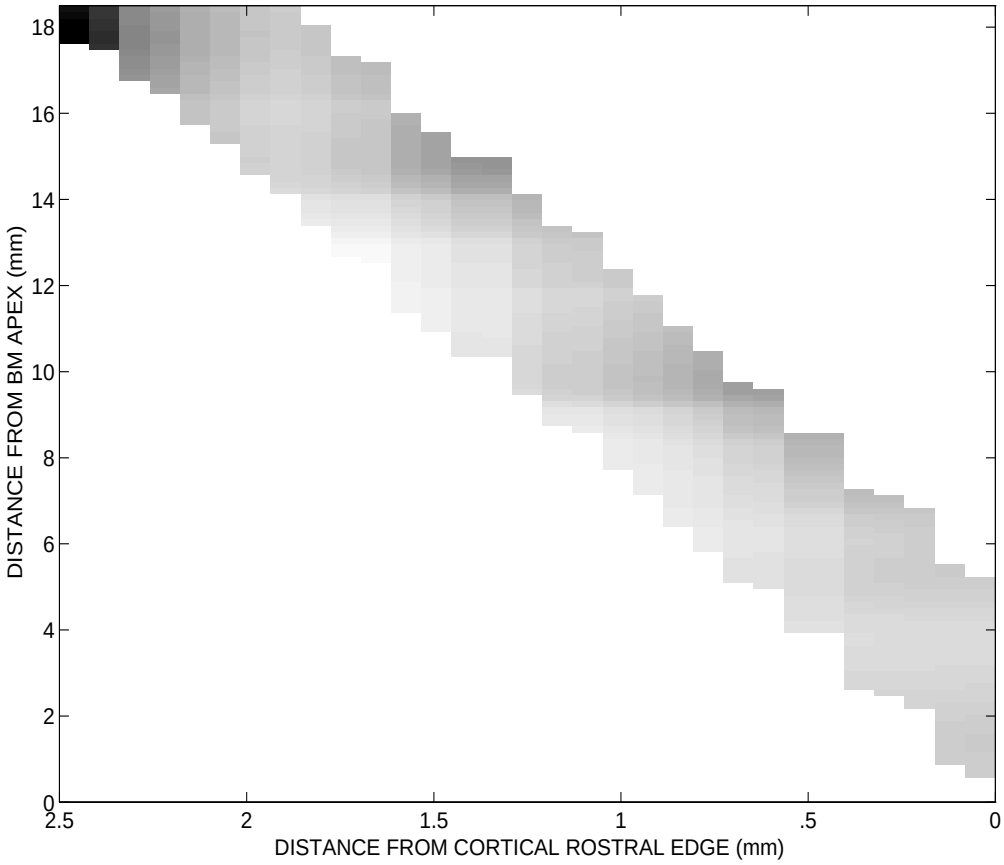
DISTANCE FROM BM APEX (mm)
18
16
14
12
10
8
6
4
2
0
2.5
2
1.5
1
.5
0
DISTANCE FROM CORTICAL ROSTRAL EDGE (mm)

FIG. 6

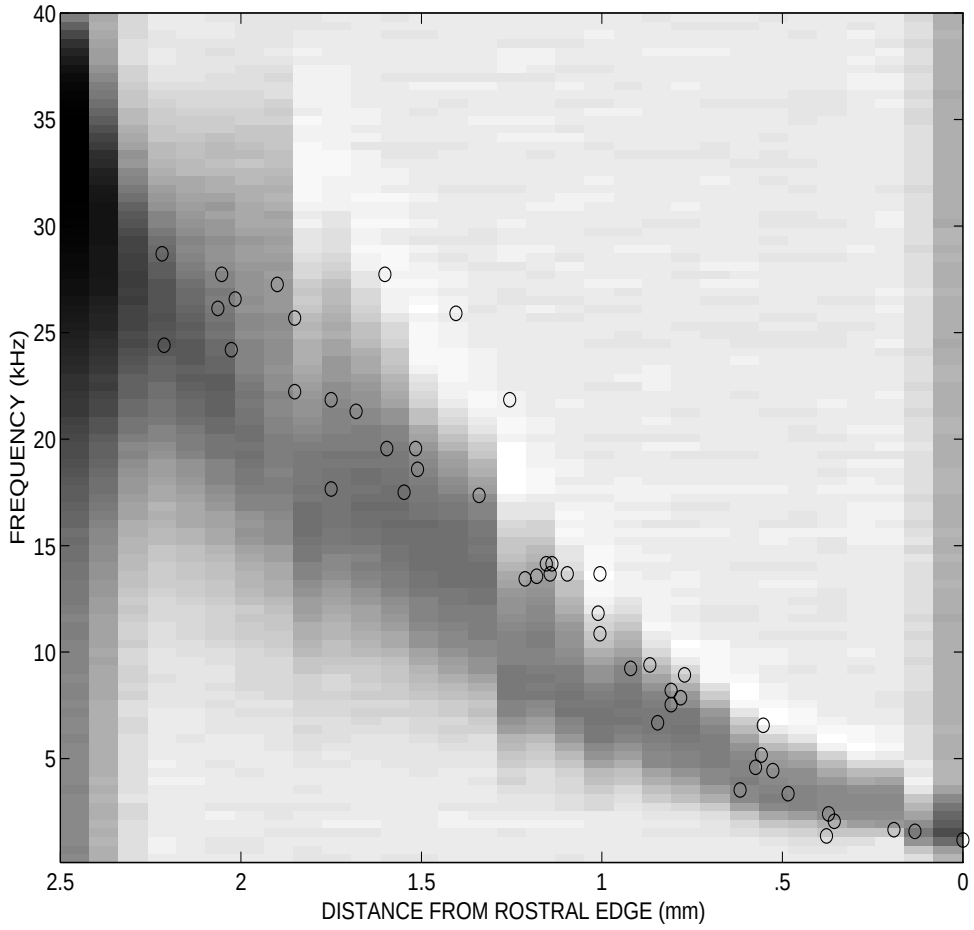
40
35
30
25
20
15
10
5
FREQUENCY (kHz)
2.5
2
1.5
1
.5
0
DISTANCE FROM ROSTRAL EDGE (mm)

FIG.7

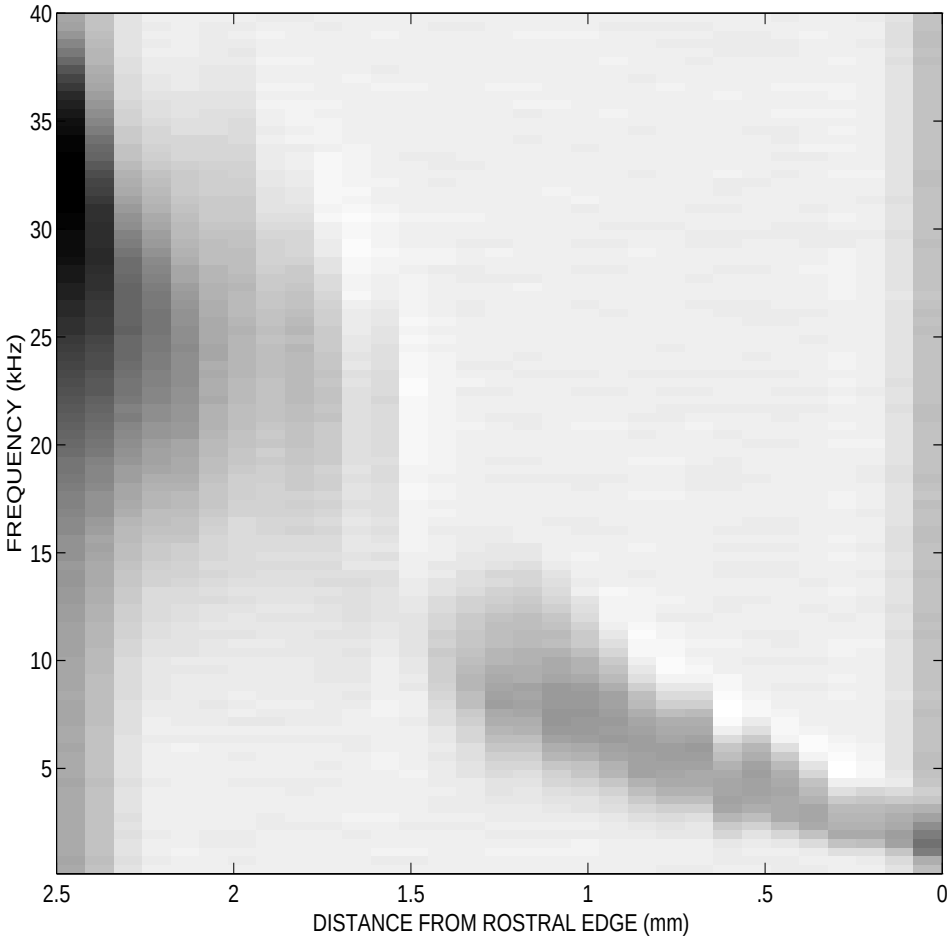
40
35
30
25
20
15
10
5
FREQUENCY (kHz)
2.5
2
1.5
1
.5
0
DISTANCE FROM ROSTRAL EDGE (mm)

FIG.8

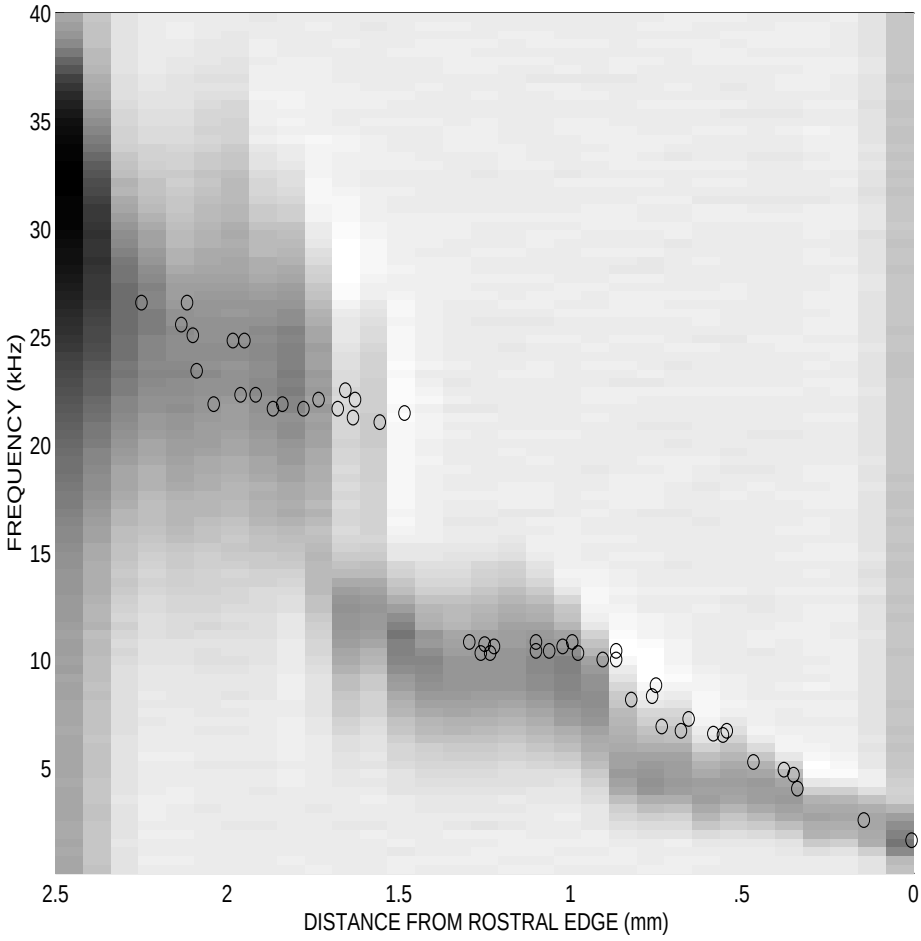
40
35
30
25
20
15
10
5
FREQUENCY (kHz)
2.5
2
1.5
1
.5
0
DISTANCE FROM ROSTRAL EDGE (mm)

FIG. 9

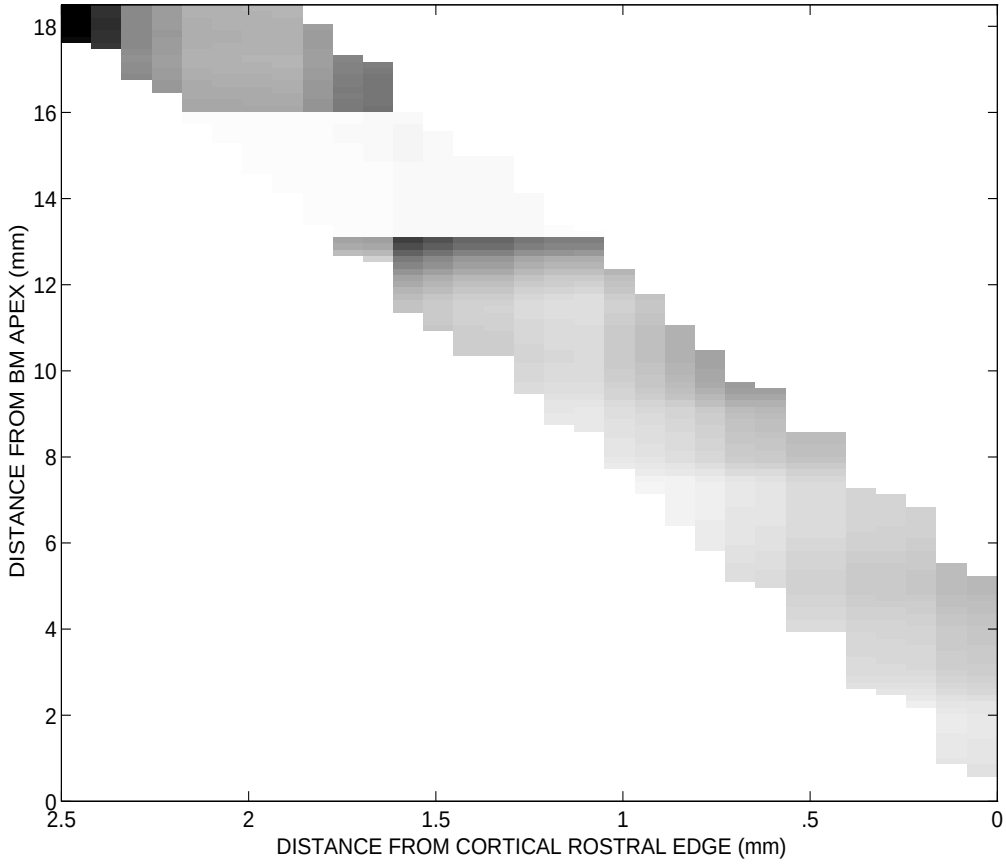
DISTANCE FROM BM APEX (mm)
18
16
14
12
10
8
6
4
2
0
2.5
2
1.5
1
.5
0
DISTANCE FROM CORTICAL ROSTRAL EDGE (mm)

FIG. 10